ELSEVIER

Journal of Organometallic Chemistry 513 (1996) 201–211

Journal of Organometallic Chemistry

Ruthenium clusters with nitrogen ligands V [1]. Pyridyl ligands on triruthenium cores. X-ray structures of $Ru_3(\mu\text{-}H)_2(\mu\text{-}NC_5H_4)_2(CO)_8$ and $Ru_3(\mu_3\text{-}\eta^2\text{-}PPhCH_2PPh_2)(\mu\text{-}NC_5H_4)(CO)_8$

Marie P. Cifuentes [a], Mark G. Humphrey [b,*], Brian W. Skelton [c], Allan H. White [c]

[a] *Department of Chemistry, University of New England, Armidale, N.S.W. 2351, Australia*
[b] *Department of Chemistry, Australian National University, Canberra, A.C.T. 0200, Australia*
[c] *Department of Chemistry, University of Western Australia, Nedlands, W.A. 6907, Australia*

Received 14 August 1995

Abstract

The reaction between $Ru_3(CO)_{12}$ and pyridine affords a mixture of $Ru_3(\mu\text{-}H)(\mu\text{-}NC_5H_4)(CO)_{10}$ (**1**) and $Ru_3(\mu\text{-}H)_2(\mu\text{-}NC_5H_4)_2(CO)_8$ (**2**). Cluster **2** is the first crystallographically-verified triruthenium cluster with two orthometalated N-heterocycles; these ligands occupy edge-bridging diaxial sites on two of the three Ru–Ru bonds, one on each side of the triruthenium plane, with the hydrido ligands bridging the same Ru–Ru bonds as the pyridyls. Reaction of **1** with dppm gives $Ru_3(\mu_3\text{-}\eta^2\text{-}PPhCH_2PPh_2)(\mu\text{-}NC_5H_4)(CO)_8$ (**3**) in low yield amongst a mixture of products. The structural study confirms that **3** results from dephenylation of the dppm ligand; concomitant loss of the hydrido ligand suggests reductive elimination of benzene. Formal electron counting on this electron precise cluster shows that Ru(1) and Ru(3) are each 0.5e deficient, and Ru(2) is 1e rich; two "semibridging" carbonyls in the triruthenium plane redistribute electron density from Ru(2) to Ru(1) and Ru(3). Reaction of $Ru_3(\mu\text{-dppm})(CO)_{10}$ with pyridine also affords **3** in low yield. Related reactions with the more flexible bidentate ligand dppe afford more complex mixtures of products. Whereas thermolysis of **1** affords $[Ru_2(\mu\text{-}H)(\mu\text{-}NC_5H_4)_2(CO)_4(NC_5H_5)_2][Ru_{10}(\mu\text{-}H)(\mu_6\text{-}C)(CO)_{24}]$, thermolyses of **2** or **3** do not lead to tractable products.

Keywords: Ruthenium; Clusters; Pyridyls; Carbonyls; Crystal structure

1. Introduction

The reactions of ruthenium clusters with nitrogen ligands are of current interest [2]. A suitable choice of nitrogen-donor molecule with a ruthenium cluster can conceivably model the heterogeneously-catalyzed hydrodenitrogenation of liquid fuels. Pyridine and its higher homologues are believed to be the most persistent N-containing impurities in liquid fuels [3]; pyridine in a variety of coordination modes is therefore of interest in these modelling studies. We have previously reported the reaction of $Ru_3(CO)_{12}$ with pyridine [4], which affords clusters containing edge-bridging pyridyl ligands, although we had no structural data at the time of that report. Subsequently, we investigated the reaction of $Ru_3(CO)_{12}$ with piperidine [5], a likely reduction intermediate of pyridine. These studies showed substantial C–N weakening on increasing the number of metals interacting with the N-heterocycle residue from two to three. Our attempts to vary the coordination of the pyridyl moiety have involved reaction of mixed-metal clusters with pyridine [6], which have afforded examples of σ-bound pyridine, and thermolysis of $Ru_3(\mu\text{-}H)(\mu\text{-}NC_5H_4)(CO)_{10}$ [7], which gave a high nuclearity cluster anion as its $[Ru_2(\mu\text{-}H)(\mu\text{-}NC_5H_4)_2(CO)_4(NC_5H_5)_2]^+$ salt; the cation contains two bridging pyridyls and two σ-bound pyridines. The synthesis of the high nuclearity cluster anion $[Ru_{10}(\mu\text{-}H)(\mu_6\text{-}C)(CO)_{24}]^-$ must involve cluster fragmentation and reaggregation; we reasoned that it should be possible to disfavour the change in cluster nuclearity by employing an edge-bridging or face-capping ligand to maintain cluster core integrity. With this in mind, we have investigated the use of the bidentate ligand bis(diphenylphosphino)-

* Corresponding author.
[1] For Part IV see Ref. [1].

SSDI 0022-328X(95)05912-1

methane (dppm); we report herein the results of our studies involving the reactions between $Ru_3(\mu\text{-}H)(\mu\text{-}NC_5H_4)(CO)_{10}$ and dppm, and between the stabilized cluster $Ru_3(\mu\text{-dppm})(CO)_{10}$ and pyridine. Included in this contribution is an X-ray study of our previously-reported edge-bridged bis(pyridyl) cluster $Ru_3(\mu\text{-}H)_2(\mu\text{-}NC_5H_4)_2(CO)_8$ [4], which has recently become available.

2. Results

2.1. X-ray structural study of 2

We have previously reported the reaction between $Ru_3(CO)_{12}$ and pyridine in refluxing cyclohexane, which affords $Ru_3(\mu\text{-}H)(\mu\text{-}NC_5H_4)(CO)_{10}$ (**1**) (96%) together with a small amount of $Ru_3(\mu\text{-}H)_2(\mu\text{-}NC_5H_4)_2(CO)_8$ (**2**) (< 1%) [4]. Laine and coworkers [8] isolated **2**, but not **1**, when carrying out this reaction in the higher boiling heptane. We have now obtained suitable crystals of **2** for an X-ray structural study, although crystals of **1** have remained elusive. An ORTEP plot of **2** is shown in Fig. 1, a summary of crystal and refinement data is found in Table 1, fractional coordinates are listed in Table 2, and selected bond lengths and angles are displayed in Table 3.

The three metal atoms form an isosceles triangle [Ru(1)–Ru(2) 2.9214(8), Ru(1)–Ru(3) 2.917(2), Ru(2)–Ru(3) 2.832(1) Å], with the longer Ru–Ru bonds bridged by hydrido and pyridyl ligands. Ru–CO [1.859(5)–1.924(5) Å, av. 1.90 Å] and RuC–O distances [1.125(6)–1.139(6) Å, av. 1.13 Å] are unexceptional. Of particular interest to hydrodenitrogenation modelling are distances within the pyridyl ligand, and any variations from non-ligated pyridine geometries; distances within the axially coordinated pyridyl ligands are "normal" (i.e. they are within the expected range of values for *N*-heterocycles, and there is no significant bond length alternation concomitant with coordination), although these ligands are disordered about the ligating *C* and *N* atoms. The hydrido atoms were located, with the Ru_2H dihedral angles at 51(2)° and 50(3)° to the plane of the triruthenium triangle. We have mentioned previously that crystallographically located hydrido ligands are rare in structures of this type; in the related piperidyl cluster $Ru_3(\mu\text{-}H)(\mu\text{-}NC_5H_8)(CO)_{10}$ [5], the hydride was unsymmetrically displaced towards the N-coordinated ruthenium [Ru–H 1.68(4), 1.94(4) Å]; in **2** H(12)–Ru(1,2) are 1.85(4), 1.72(4) and H(13)–Ru(1,3) 1.73(4), 1.72(4) Å.

Cluster **2** is the first crystallographically-verified triruthenium cluster with two orthometalated *N*-heterocycles; these ligands occupy edge-bridging diaxial sites on two of the three Ru–Ru bonds, one on each side of the triruthenium plane, with the overall molecular symmetry being a good approximation to **2**. To ascertain the effect of orthometalated cluster ligation of the *N*-heterocycle on bonding distances, the M_2NC distances for **2** and related ruthenium and osmium complexes are listed in Table 4. It is immediately apparent that no unsupported (apart from the heterocycle residue) M–M linkage has been structurally characterized; all previously reported examples carry a hydrido ligand (which lengthens the M–M bond), making meaningful discussion of variation in this parameter difficult given the impossibility of deconvoluting the individual contributions. The pyridyl-bridged M–M distances in **2** fall in the centre of the range of previously reported values. The M–N and M–C distances seem very flexible, spanning large ranges [2.002(2)–2.143(4) Å, av. 2.10 Å and 2.087(4)–2.143(4)

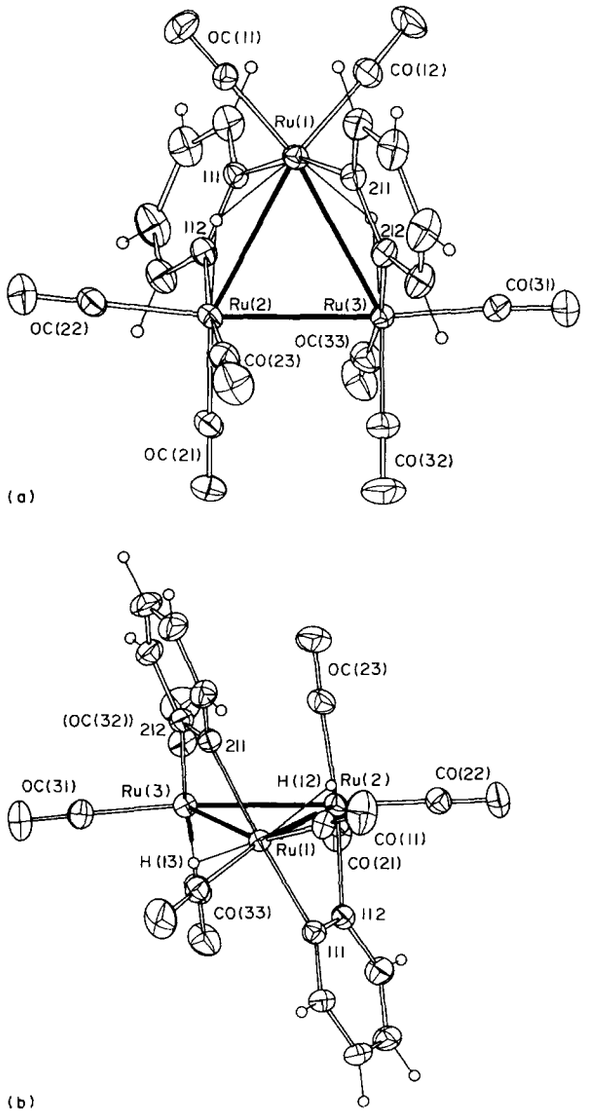

Fig. 1. Molecular structure and atomic labelling scheme for $Ru_3(\mu\text{-}H)_2(\mu\text{-}NC_5H_4)_2(CO)_8$ (**2**). 20% thermal ellipsoids are shown for the non-hydrogen atoms; hydrogen atoms have arbitrary radii of 0.1 Å. Projections are shown (a) normal and (b) oblique to the Ru_3 plane.

Table 1
Summary of crystallographic data for $Ru_3(\mu\text{-}H)_2(\mu\text{-}NC_5H_4)_2(CO)_8$ (**2**) and $Ru_3(\mu_3\text{-}\eta^2\text{-}PPhCH_2PPh_2)(\mu\text{-}NC_5H_4)(CO)_8$ (**3**)

	2	**3**
Formula	$C_{18}H_{10}N_2O_8Ru_3$	$C_{32}H_{21}NO_8P_2Ru_3$
M	685.5	912.7
Crystal system	monoclinic	monoclinic
Space group	$P2_1/c$ (No. 14)	$P2_1/c$
a (Å)	15.171(3)	9.763(3)
b (Å)	8.935(5)	35.800(13)
c (Å)	16.302(4)	10.837(2)
β (°)	93.72(2)	122.32(2)
V (Å^3)	2205	3201
$D_{calc.}$ (g cm^{-3})	2.07	1.89
Z	4	4
μ_{Mo} (cm^{-1})	18.8	15.5
Specimen (mm^3)	0.37 × 0.65 × 0.16	0.05 × 0.15 × 0.42
$A^*_{min,max}$	1.34, 1.90	1.08, 1.26
$2\theta_{max}$ (°)	50	50
N	3870	5615
N_0	3525	3003
R	0.029	0.046
R_w	0.037	0.042

Table 2
Non-hydrogen atom coordinates and equivalent isotropic displacement parameters for $Ru_3(\mu\text{-}H)_2(\mu\text{-}NC_5H_4)_2(CO)_8$ (**2**)

Atom	x	y	z	U_{eq} (Å^2)
Ru(1)	0.24616(2)	0.52980(4)	0.23794(2)	0.0375(1)
Ru(2)	0.28269(2)	0.44344(4)	0.40963(2)	0.0422(1)
Ru(3)	0.22818(2)	0.22136(4)	0.29317(2)	0.0418(1)
C(11)	0.3050(3)	0.7092(5)	0.2227(3)	0.056(2)
O(11)	0.3423(3)	0.8171(4)	0.2123(3)	0.100(2)
C(12)	0.1831(3)	0.5515(5)	0.1357(3)	0.058(2)
O(12)	0.1452(3)	0.5695(5)	0.0749(2)	0.101(2)
C(21)	0.2387(3)	0.3247(6)	0.4954(3)	0.054(2)
O(21)	0.2119(3)	0.2540(4)	0.5458(2)	0.082(2)
C(22)	0.3255(3)	0.6071(6)	0.4778(3)	0.058(2)
O(22)	0.3501(3)	0.7026(5)	0.5186(3)	0.093(2)
C(23)	0.3927(3)	0.3363(6)	0.4102(3)	0.063(2)
O(23)	0.4585(2)	0.2751(5)	0.4101(3)	0.096(2)
C(31)	0.1829(3)	0.0858(5)	0.2090(3)	0.059(2)
O(31)	0.1539(3)	0.0003(5)	0.1643(2)	0.091(2)
O(32)	0.3103(3)	−0.0222(5)	0.4031(3)	0.110(2)
C(32)	0.2806(3)	0.0687(6)	0.3618(3)	0.064(2)
C(33)	0.1232(3)	0.2251(6)	0.3516(3)	0.063(2)
O(33)	0.0592(2)	0.2267(5)	0.3834(2)	0.091(2)
N(111) *	0.1502(2)	0.6192(4)	0.3123(2)	0.043(1)
C(111) *	0.1502(2)	0.6192(4)	0.3123(2)	0.043(1)
N(112) *	0.1636(2)	0.5668(4)	0.3894(2)	0.049(1)
C(112) *	0.1636(2)	0.5668(4)	0.3894(2)	0.049(1)
C(113)	0.1062(3)	0.6119(6)	0.4472(3)	0.064(2)
C(114)	0.0381(3)	0.7060(7)	0.4288(3)	0.076(2)
C(115)	0.0264(3)	0.7614(6)	0.3496(4)	0.074(2)
C(116)	0.0828(3)	0.7151(6)	0.2921(3)	0.062(2)
N(211) *	0.3447(2)	0.3953(4)	0.1931(2)	0.046(1)
C(211) *	0.3447(2)	0.3953(4)	0.1931(2)	0.046(1)
N(212) *	0.3430(2)	0.2601(4)	0.2261(2)	0.044(1)
C(212) *	0.3430(2)	0.2601(4)	0.2261(2)	0.044(1)
C(213)	0.4064(3)	0.1582(5)	0.2093(3)	0.066(2)
C(214)	0.4718(3)	0.1939(7)	0.1579(4)	0.079(2)
C(215)	0.4728(3)	0.3323(7)	0.1226(4)	0.076(2)
C(216)	0.4095(3)	0.4322(6)	0.1405(3)	0.059(2)

* Site occupancy factor 0.5.

Table 3
Selected bond lengths (Å) and angles (°) for $Ru_3(\mu\text{-}H)_2(\mu\text{-}NC_5H_4)_2(CO)_8$ (**2**). X is the C/N composite. In this and Table 4 the entries for the two halves of the molecules related by the putative two-fold axis are laid out in parallel

Ru(1)–Ru(2)	2.9214(8)		
Ru(1)–Ru(3)	2.917(2)		
Ru(2)–Ru(3)	2.832(1)		
C–O	1.125(6)–1.139(6)		
Ru(1)–C(11)	1.859(5)	Ru(1)–C(12)	1.877(5)
Ru(1)–X(111)	2.111(4)	Ru(1)–X(211)	2.087(6)
Ru(2)–C(21)	1.910(5)	Ru(3)–C(32)	1.905(5)
Ru(2)–C(22)	1.923(5)	Ru(3)–C(31)	1.923(5)
Ru(2)–C(23)	1.924(5)	Ru(3)–C(33)	1.908(5)
Ru(2)–X(112)	2.124(4)	Ru(3)–X(212)	2.143(4)
X(111)–X(112)	1.344(5)	X(211)–X(212)	1.323(5)
X(111)–C(116)	1.358(6)	X(211)–C(216)	1.386(9)
X(112)–C(113)	1.384(6)	X(212)–C(213)	1.366(6)
C(113)–C(114)	1.350(7)	C(213)–C(214)	1.376(8)
C(114)–C(115)	1.383(8)	C(214)–C(215)	1.364(9)
C(115)–C(116)	1.375(7)	C(215)–C(216)	1.357(7)
Ru(2)–Ru(1)–Ru(3)	58.04(1)	X(111)–Ru(1)–X(211)	162.8(1)
Ru(1)–Ru(2)–Ru(3)	60.91(3)	Ru(1)–Ru(3)–Ru(2)	61.05(3)
Ru(3)–Ru(1)–X(211)	69.4(2)	Ru(2)–Ru(1)–X(111)	69.19(9)
Ru(1)–Ru(2)–X(112)	66.9(1)	Ru(1)–Ru(3)–X(212)	66.1(2)
R–C–O	174.9(5)–179.4(4)		
Ru(1)–X(111)–X(112)	109.7(3)	Ru(1)–X(211)–X(212)	110.4(2)
X(112)–X(111)–C(116)	120.8(4)	X(212)–X(211)–C(216)	120.2(4)
Ru(1)–X(111)–C(116)	129.5(3)	Ru(1)–X(211)–C(216)	129.2(3)
Ru(2)–X(112)–C(113)	127.7(3)	Ru(3)–X(212)–C(213)	127.0(3)
X(111)–X(112)–C(113)	118.1(4)	X(211)–X(212)–C(213)	119.6(4)
Ru(2)–X(112)–X(111)	113.7(3)	Ru(3)–X(212)–X(211)	113.2(3)
X(112)–C(113)–C(114)	122.4(4)	X(212)–C(213)–C(214)	120.8(5)
C(113)–C(114)–C(115)	118.7(5)	C(213)–C(214)–C(215)	119.7(5)
C(114)–C(115)–C(116)	118.7(5)	C(214)–C(215)–C(216)	118.6(5)
C(115)–C(116)–X(111)	121.1(5)	C(215)–C(216)–X(211)	121.1(5)

Å, av. 2.12 Å], with a large number of examples having symmetrically disposed *C*, *N*-coordinated heterocycle residues which are possibly disordered about the C(2) and N atoms; examples exist of residues containing shorter M–C or shorter M–N linkages. Not surprisingly, the C–N bond [1.312(0)–1.383 Å, av. 1.34 Å] in these complexes is substantially longer than that in comparable edge-bridged, non-aromatic, *C–N* systems (av. 1.27 Å), and comparable in length to that of face-capped, non-aromatic, *C–N* systems (av. 1.35 Å) [5]. Extending our observations with the piperidyl system, face-capping coordination of the pyridyl ligand should weaken the coordinated C–N bond significantly, perhaps to that of a formal single bond. In previous

Table 4

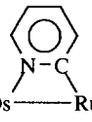

Complex	M–M	M–N	M–C	C–N	Other M–M bridge	Reference
$Ru_3(\mu_3\text{-}\eta^2\text{-}PPhCH_2PPh_2)(\mu\text{-}NC_5H_4)(CO)_8$ (**3**)	2.782(1)	2.12(1)	2.10(2)	1.35(1)	(μ-CO) (μ_3-η^2-$PPhCH_2PPh_2$)	This work
$Ru_3(\mu\text{-}H)(\mu\text{-}C_{13}H_8N)(CO)_{10}$	2.866(1)	2.133(1)	2.133(1)	1.312(0)	(μ-H)	[25]
$Os_3(\mu\text{-}H)(\mu\text{-}C_9H_6N)(CO)_{10}$	2.909(2)	[a]	[a]	1.329(35) [b]	(μ-H)	[8]
$Os_3(\mu\text{-}H)(\mu\text{-}\eta^3\text{-}C_5H_3N\text{-}2\text{-}CH{=}NPr^i)(CO)_9$	2.911(2)	2.002(2)	2.12(2)	1.33(2)	(μ-H)	[26]
$Ru_3(\mu\text{-}H)(\mu\text{-}NC_5H_4)(CO)_9(PPh_3)$	2.916(1)	2.103(6)	2.106(6)	1.33(1)	(μ-H)	[6]
$Ru_3(\mu\text{-}H)_2(\mu\text{-}NC_5H_4)_2(CO)_8$ (**2**) [c]	2.917(2)	2.087(4)/	2.143(4)	1.323(5)	(μ-H)	This work
	2.9214(8)	2.111(4)/	2.124(4)	1.344(5)	(μ-H)	
$Os_3(\mu\text{-}H)_2(\mu\text{-}C_9H_6N)_2(CO)_8$	2.92(1)	[a]	[a]	1.367–1.383 [b]	(μ-H)	[8]
$Os_3(\mu\text{-}H)(\mu\text{-}\eta^3\text{-}C_{10}H_7N_2)(CO)_9$	2.926(4)	2.058(9)	2.118(12)	1.352(14)	(μ-H)	[27]

[a] Not reported. [b] Reported in Ref. [25]. [c] Two independent pyridyl groups, both N, C disordered.

work, we have shown that thermolysis of **1** does not afford a face-capping pyridyl ligand (as occurs in thermolysis of μ-piperidyl), but rather to a complex rearrangement leading to $[Ru_2(\mu\text{-H})(\mu\text{-}NC_5H_4)_2(CO)_4(NC_5H_5)_2][Ru_{10}(\mu\text{-H})(\mu_6\text{-C})(CO)_{24}]$ [7]. It seems logical to investigate a similar reaction on a cluster which would resist this rearrangement; our initial investigations have focussed on clusters with bidentate ligands.

2.2. Synthesis and spectroscopic characterization of 3

The reaction between $Ru_3(\mu\text{-H})(\mu\text{-}NC_5H_4)(CO)_{10}$ (**1**) and bis(diphenylphosphino)methane (dppm) in cyclohexane at 50°C was found to give a complex mixture of products; separation by thin layer chromatography and crystallization afforded unreacted **1**, $Ru_3(\mu\text{-dppm})(CO)_{10}$, $Ru_3(\mu\text{-dppm})_2(CO)_8$, and orange crystals identified as $Ru_3(\mu_3\text{-}\eta^2\text{-}PPhCH_2PPh_2)(\mu\text{-}NC_5H_4)(CO)_8$ (**3**), together with copious amounts of material on the baseline. Product **3** is derived from **1** by dephenylation and orthometalation of the pyridine and elimination of the hydrido ligand; the fragments presumably leave as benzene, although this was not verified. Compound **3** was characterized by the usual spectroscopic methods. The ^{1}H NMR spectrum shows the expected resonances between 8.25 and 6.78 ppm corre-

Table 5
Non-hydrogen atom coordinates and equivalent isotropic displacement parameters for $Ru_3(\mu_3\text{-}\eta^2\text{-}PPhCH_2PPh_2)(\mu\text{-}NC_5H_4)(CO)_8$ (**3**)

Atom	x	y	z	U_{eq} (Å^2)
Ru(1)	0.5091(1)	0.61086(2)	−0.2220(1)	0.0357(5)
Ru(2)	0.7170(1)	0.58831(2)	0.0659(1)	0.0381(5)
Ru(3)	0.7258(1)	0.66385(2)	−0.0274(1)	0.0368(5)
C(11)	0.469(1)	0.6402(3)	−0.380(1)	0.044(7)
O(11)	0.442(1)	0.6573(2)	−0.4783(9)	0.069(6)
C(12)	0.312(2)	0.5847(3)	−0.341(1)	0.055(7)
O(12)	0.190(1)	0.5702(3)	−0.408(1)	0.082(6)
C(21)	0.825(2)	0.5484(3)	0.197(1)	0.062(8)
O(21)	0.895(1)	0.5244(2)	0.276(1)	0.085(6)
C(22)	0.522(1)	0.5590(3)	−0.063(1)	0.048(7)
O(22)	0.427(1)	0.5359(2)	−0.0971(9)	0.064(5)
C(23)	0.904(1)	0.6211(3)	0.190(1)	0.046(7)
O(23)	1.027(1)	0.6303(2)	0.2851(9)	0.070(5)
C(31)	0.907(1)	0.6522(3)	−0.044(1)	0.047(7)
O(31)	1.011(1)	0.6469(2)	−0.063(1)	0.071(6)
C(32)	0.808(1)	0.6981(3)	0.133(1)	0.054(8)
O(32)	0.856(1)	0.7200(2)	0.223(1)	0.074(6)
C(33)	0.662(1)	0.7016(3)	−0.167(1)	0.045(7)
O(33)	0.624(1)	0.7246(2)	−0.2517(9)	0.070(6)
P(1)	0.5700(4)	0.61312(8)	0.1671(3)	0.038(2)
C(111)	0.678(1)	0.6436(3)	0.326(1)	0.040(6)
C(112)	0.626(1)	0.6785(3)	0.338(1)	0.051(7)
C(113)	0.711(2)	0.6983(3)	0.469(2)	0.062(9)
C(114)	0.844(2)	0.6832(4)	0.588(1)	0.058(8)
C(115)	0.894(2)	0.6484(4)	0.579(1)	0.062(8)
C(116)	0.814(1)	0.6291(3)	0.449(1)	0.050(7)
C(121)	0.477(1)	0.5810(3)	0.231(1)	0.038(6)
C(122)	0.378(1)	0.5945(3)	0.275(1)	0.044(7)
C(123)	0.310(1)	0.5716(3)	0.331(1)	0.051(7)
C(124)	0.343(1)	0.5341(4)	0.346(1)	0.057(7)
C(125)	0.439(2)	0.5197(3)	0.298(1)	0.063(8)
C(126)	0.505(1)	0.5427(3)	0.241(1)	0.055(8)
C(0)	0.400(1)	0.6404(3)	0.025(1)	0.047(7)
P(2)	0.4544(3)	0.65579(7)	−0.1054(3)	0.036(1)
C(211)	0.328(1)	0.6971(3)	−0.192(1)	0.038(6)
C(212)	0.228(1)	0.7000(3)	−0.340(1)	0.051(7)
C(213)	0.153(2)	0.7337(4)	−0.405(1)	0.068(8)
C(214)	0.177(2)	0.7636(4)	−0.319(2)	0.07(1)
C(215)	0.270(2)	0.7613(3)	−0.170(2)	0.071(9)
C(216)	0.349(1)	0.7282(3)	−0.106(1)	0.056(7)
N(1)	0.702(1)	0.5790(2)	−0.206(1)	0.038(5)
C(2)	0.805(1)	0.5704(3)	−0.064(1)	0.044(6)
C(3)	0.952(1)	0.5535(3)	−0.022(1)	0.047(7)
C(4)	0.990(1)	0.5464(3)	−0.126(2)	0.058(8)
C(5)	0.883(2)	0.5545(3)	−0.268(1)	0.053(8)
C(6)	0.739(1)	0.5713(3)	−0.305(1)	0.049(7)

sponding to the pyridyl and phosphine protons, as well as doublet of triplet signals at 3.58 and 3.03 ppm [J(HP) = 15 Hz, J(HH) = 5 Hz] due to the methylene protons of the dppm residue. No metal-bound hydride signal was observed. The ^{13}C NMR spectrum shows a broad signal at 206.0 ppm due to the carbonyl groups. Resonances at 154.5, 136.5 and 119.5 ppm can be assigned to carbons 6, 3 and 5 of the pyridyl moiety, respectively; the metal-bound carbon was not detected, and the signal due to C4 occurs in the phosphine carbon region 131.9–128.6 ppm. The ^{31}P NMR spectrum contains two doublets at 136.5 and 15.3 ppm showing phosphorus–phosphorus coupling of 134 Hz. The structure was confirmed by an X-ray crystallographic study. A summary of crystal and refinement data is found in Table 1, fractional coordinates of non-hydrogen atoms are given in Table 5, and selected bond distances and angles are listed in Table 6. An ORTEP plot showing the molecular geometry and atomic numbering scheme is shown in Fig. 2.

2.3. X-ray structural study of 3

The three ruthenium atoms define an isosceles triangle [Ru(1)–Ru(2) 2.782(1), Ru(1)–Ru(3) 2.784(1), Ru(2)–Ru(3) 2.904(2) Å]; the shorter Ru–Ru linkages are spanned by the edge-bridging orthometalated pyridyl moiety, or the phosphido component of the face-capping $PPhCH_2PPh_2$ group respectively. The coordination is completed by six terminally ligated carbonyl ligands and two edge-bridging carbonyls. Distances Ru–CO [1.86(1)–1.92(1) Å, av. 1.89 Å] and RuC–O [1.13(1)–1.15(1) Å, av. 1.14 Å] involving the terminal carbonyl ligands are not unusual. The other two carbonyl ligands are "semibridging" (see below); they have Ru(2)–CO distances [Ru(2)–C(22) 1.96(1), Ru(2)–C(23) 1.98(1) Å] somewhat longer than the terminal CO distances above, and weak interactions [Ru(1)–C(22) 2.49(1), Ru(3)–C(23) 2.56(1) Å] to the other metals. Angles Ru(2)–C(22)–O(22) [158(1)°] and Ru(2)–C(23)–O(23) [159(1)°] are consistent with this, being about midway between terminal (180°) and symmetrically bridging (around 133° for Ru–Ru 2.8 Å, Ru–C 1.9 Å) geometries. Distances and angles within the P-bound phenyl groups and the N-heterocycle are unexceptional. Other cluster bonding parameters are discussed below.

The presence of the semibridging interactions is readily explicable by electron counting. Overall, **3** is an

Table 6
Selected bond lengths (Å) and angles (°) for $Ru_3(\mu_3\text{-}\eta^2\text{-}PPhCH_2PPh_2)(\mu\text{-}NC_5H_4)(CO)_8$ (**3**)

Ru(1)–Ru(2)	2.782(1)	Ru(1)–Ru(3)	2.784(1)
Ru(2)–Ru(3)	2.904(2)	Ru(1)–C(11)	1.86(1)
Ru(1)–C(12)	1.89(1)	Ru(1)–C(22)	2.49(1)
Ru(1)–P(2)	2.278(4)	Ru(1)–N(1)	2.12(1)
Ru(2)–C(21)	1.89(1)	Ru(2)–C(22)	1.96(1)
Ru(2)–C(23)	1.98(1)	Ru(2)–P(1)	2.395(4)
Ru(2)–C(2)	2.10(2)	Ru(3)–C(23)	2.56(1)
Ru(3)–C(31)	1.92(2)	Ru(3)–C(32)	1.92(1)
Ru(3)–C(33)	1.87(1)	Ru(3)–P(2)	2.328(4)
C–O	1.13(1)–1.15(1)	P(1)–C(0)	1.829(9)
C(0)–P(2)	1.84(2)	N(1)–C(2)	1.35(1)
N(1)–C(6)	1.34(2)	C(2)–C(3)	1.39(2)
C(3)–C(4)	1.38(2)	C(4)–C(5)	1.35(2)
C(5)–C(6)	1.38(2)		
Ru(2)–Ru(1)–Ru(3)	62.91(4)	Ru(2)–Ru(1)–P(2)	80.17(7)
Ru(2)–Ru(1)–N(1)	70.6(3)	Ru(3)–Ru(1)–P(2)	53.63(8)
Ru(1)–Ru(2)–Ru(3)	58.59(3)	Ru(1)–Ru(2)–P(1)	98.60(7)
Ru(1)–Ru(2)–C(2)	69.7(3)	Ru(3)–Ru(2)–P(1)	87.17(8)
Ru(1)–Ru(3)–Ru(2)	58.50(3)	Ru(1)–Ru(3)–P(2)	52.00(8)
Ru(2)–Ru(3)–P(2)	76.78(7)	Ru(1)–C(11)–O(11)	178.2(9)
Ru(1)–C(12)–O(12)	176(1)	Ru(2)–C(21)–O(21)	178(2)
Ru(1)–C(22)–O(22)	125.7(7)	Ru(2)–C(22)–O(22)	158(1)
Ru(2)–C(23)–O(23)	159(1)	Ru(3)–C(23)–O(23)	122.1(9)
Ru(3)–C(31)–O(31)	175(1)	Ru(3)–C(32)–O(32)	176(1)
Ru(3)–C(33)–O(33)	180(1)	Ru(2)–P(1)–C(0)	107.9(5)
P(1)–C(0)–P(2)	107.7(7)	Ru(1)–P(2)–Ru(3)	74.4(1)
Ru(1)–P(2)–C(0)	117.6(4)	Ru(3)–P(2)–C(0)	119.9(3)
Ru(1)–N(1)–C(2)	107.9(9)	Ru(1)–N(1)–C(6)	130.9(7)
C(2)–N(1)–C(6)	121(1)	Ru(2)–C(2)–N(1)	111.5(9)
Ru(2)–C(2)–C(3)	129.5(9)	N(1)–C(2)–C(3)	119(1)
C(2)–C(3)–C(4)	120(1)	C(3)–C(4)–C(5)	121(1)
C(4)–C(5)–C(6)	118(2)	N(1)–C(6)–C(5)	122(1)

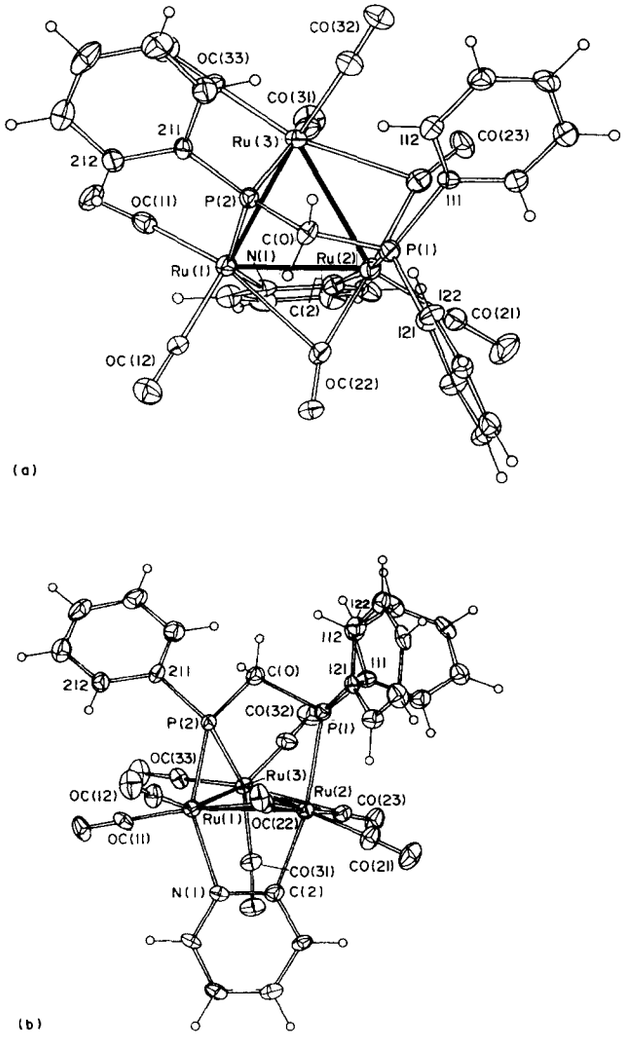

Fig. 2. Molecular structure and atomic labelling scheme for $Ru_3(\mu_3\text{-}\eta^2\text{-}PPhCH_2PPh_2)(\mu\text{-}NC_5H_4)(CO)_8$ (**3**). 20% thermal ellipsoids are shown for the non-hydrogen atoms; hydrogen atoms have arbitrary radii of 0.1 Å. Projections are shown (a) normal and (b) oblique to the Ru_3 plane.

electron precise 48 CVE triangular cluster [3 × 8(Ru) + 5($PPhCH_2PPh_2$) + 3(NC_5H_4) + 8 × 2(CO)]. However, in the absence of "semibridging" carbonyls, the metal atoms individual electron counts would be Ru(1) (17.5e), Ru(2) (19e) and Ru(3) (17.5e). The semibridging interactions thus serve to redistribute electron density from the electron rich Ru(2) to the comparatively electron poor Ru(1) and Ru(3). Curtis [9] has defined an "asymmetry parameter", $\alpha = (d_2 - d_1)/d_1$, where d_2 is the long M · · · C distance and d_1 is the short M–C distance in one $M_2(CO)$ fragment. For Ru(1)Ru(2)CO(22), α = 0.21, and for Ru(3)Ru(2)CO(23), α = 0.23; both values lie in the middle of the range $0.1 < \alpha < 0.6$ which Curtis regards as the "semibridging" regime. Cotton et al. [10] (**A**) and Curtis [9] (**B**) have suggested two main types of "semibridging" carbonyl group in metal–metal bonded complexes:

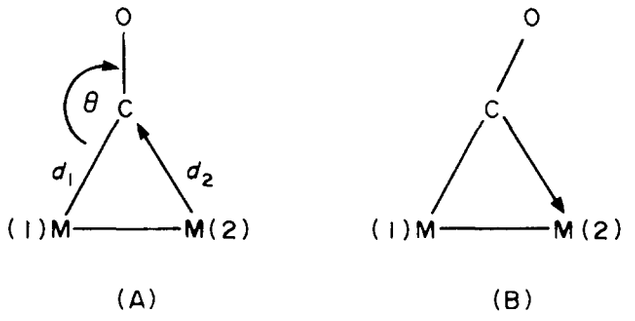

Type **A** relieves charge imbalance by back-donation of electrons from electron-rich M(2) into the π^* orbitals of the "semibridging" carbonyl. Type **B** involves electron donation from the CO π orbitals to M(2) to relieve electron deficiency at M(2). The present examples have structural type **A**, but electronic situation **B** [i.e. electron deficiency at M(2)], and may therefore be regarded as anomalous. The reason that **3** does not adopt structural type **B** may be steric; in the absence of the bridging carbonyls, Ru(1) and Ru(3) are 6-coordinate and Ru(2) is 5-coordinate. "Semibridging" carbonyls are comparatively unusual; a Cambridge Structural Database survey revealed 20 examples of triruthenium cores with at least two bridging carbonyls. Of these, only two clusters contain semibridging interactions, one of which is marginal ($\{Ru_3(\mu\text{-}\eta^2\text{-}CN)(\mu\text{-}CO)_3(CO)_7\}_2$ [11] where α = 0.13). In the more clearcut example, $Ru_3(\mu_3\text{-}\eta^2\text{-}PPhNC_5H_4)(\mu\text{-}PPh_2)(\mu\text{-}CO)_2(CO)_5(PPh_3)$ [12], one of the Ru(μ-CO)Ru units has α = 0.21 and ∠ Ru–C–O 154.2(6)°; the "semibridging" carbonyl interaction is thus similar to that in **3**.

Assignment of C(1) and N(2) was based on thermal parameters and refinement, and is necessarily cautious (being mindful of the extensive list of disordered *C*, *N*-orthometalated heterocycles reported previously). However, given the asymmetry in electron distribution, the alternative assignment is much less likely, as it leads to an even greater polarization of electron density [result: Ru(1) 16.5e, Ru(2) 20e, Ru(3) 17.5e]. The assignment of C(1) and N(2) herein is the more plausible on both crystallographic and chemical grounds.

The $Ru_3(PPhCH_2PPhR)$ core distances for **3**, and for previously reported examples of triruthenium complexes containing the ($\mu_3\text{-}\eta^2\text{-}PPhCH_2PPhR$) group, are collected in Table 7. Ru(1)–Ru(3) is much shorter in **3** than in the other examples. As Ru(1)–P(2) and Σ[Ru(3)–P(2) + Ru(1)–P(2)] are also shorter than other examples, it seems that the Ru(3)Ru(1)P(2) unit contracts in **3** to ameliorate the comparative electron defi-

Table 7

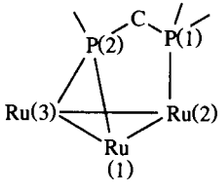

Complex	Ru(1)–Ru(3)	Ru(2)–Ru(3)	Ru(1)–Ru(2)	Ru(3)–P(2)	Ru(1)–P(2)	Ru(2)–P(1)	Reference
$Ru_3(\mu\text{-}NC_5H_4)(\mu_3\text{-}\eta^2\text{-}PPhCH_2PPh_2)(CO)_8$ (**3**)	2.784(1)	2.904(2) [d]	2.782(1) [d,h]	2.328(4)	2.278(4)	2.395(4)	This work
$Ru_3(\mu\text{-}H)(\mu_3\text{-}\eta^2\text{-}PPhCH_2PPh_2)(CO)_9$	2.820(1)	2.890(1)	3.012(1) [c]	2.306(1)	2.332(1)	2.384(1)	[20]
$Ru_3(\mu\text{-}C_4H_2Ph_2)(\mu_3\text{-}\eta^2\text{-}PPhCH_2PPhC_6H_4)(CO)_6$	2.827(4)	2.982(3) [f]	2.714(3) [g]	2.288(6)	2.352(7)	2.360(7)	[14]
$Ru_3(\mu\text{-}H)_2(\mu_3\text{-}\eta^2\text{-}PPhCH_2PPh_2)_2(CO)_6$	2.8361(2) [c]	2.8361(2) [i]	3.0367(5) [c]	2.2958(6)	2.3262(6)	2.3863(6)	[28]
$Ru_3(\mu\text{-}CuPPh_3)(\mu_3\text{-}\eta^2\text{-}PPhCH_2PPh_2)(CO)_9$	2.885(1) [l]	2.873(1)	2.896(1)	2.336(2)	2.316(2)	2.415(2)	[18]
$Ru_3(\mu\text{-}\eta^3\text{-}C_3H_5)(\mu_3\text{-}\eta^2\text{-}PPhCH_2PPh_2)(CO)_8$	2.887(1) [e]	2.853(1) [d]	2.853(1) [d]	2.344(1)	2.359(1)	2.411(1)	[29]
$Ru_3(\mu_3\text{-}\eta^3\text{-}PPh_2CH_2PPhC_6H_4)(CO)_9$ [a]	2.888(1)	2.853(1) [f]	2.818(1)	2.347(1)	2.293(1)	2.351(1)	[20]
$Ru_3(\mu_3\text{-}\eta^3\text{-}PPh_2CH_2PPhC_6H_4)(CO)_9$ [b]	2.8962(7)	2.8618(7) [f]	2.8250(7)	2.349(1)	2.303(1)	2.359(1)	[30]
$Ru_3(\mu\text{-}AuPPh_3)(\mu_3\text{-}\eta^2\text{-}PPhCH_2PPh_2)(CO)_9$	2.942(1) [j]	2.867(1)	2.891(1)	2.348(2)	2.320(2)	2.419(2)	[18]
$Ru_3(\mu\text{-}AgPPh_3)(\mu_3\text{-}\eta^2\text{-}PPhCH_2PPh_2)(CO)_9$	2.944(1) [k]	2.873(1)	2.894(1)	2.349(2)	2.328(2)	2.432(2)	[18]

[a] Structure determination at 188 K. [b] Structure determination at 285 K. [c] (μ-H). [d] (μ-CO). [e] (μ-C_3H_5). [f] (μ-C_6H_4). [g] (μ-CPhCHCHCPh). [h] (μ-NC_5H_4). [i] (μ_3-$PPhCH_2PPh_2$): Ru(2)≡Ru(3). [j] (μ-$AuPPh_3$). [k] (μ-$AgPPh_3$). [l] (μ-$CuPPh_3$).

ciency at Ru(3) and Ru(1). Ru(1)–Ru(2) is by far the shortest pyridyl-bridged M–M linkage reported thus far (see Table 4), although the fact that all other examples are also (μ-H) bridged makes comparison difficult. $Ru_3(\mu_3\text{-}\eta^2\text{-}PPhCH_2PPh_2)(\mu\text{-}\eta^3\text{-}C_3H_5)(CO)_8$ is the complex most closely related to **3**; it has the same composition, but with an allyl rather than pyridyl group as the 3e donor. In the allyl cluster, the diequatorial-ligated allyl group symmetrically bridges Ru(1)–Ru(3), rendering all rutheniums electron precise. Although (μ-pyridyl) prefers diaxial coordination, its location on Ru(1)–Ru(2) is unexpected, as a structure with this group bridging Ru(1)–Ru(3) in diaxial sites can be drawn which would render all rutheniums electron precise. The reason for the anomaly may lie with the electronegative nitrogen and strong acceptor, orthometalated carbon positioning themselves approximately *trans* to differing phosphorus donor atoms in order to maximize electron acceptance.

3. Discussion

Other chemistry in this system has afforded less clear results. Thermolysis of a solution of **3** leads to extensive decomposition and no tractable products. Reaction of **1** with bis(diphenylphosphino)ethane (dppe) affords a more complex mixture of products than observed with dppm [13]; spectral characterization has suggested the presence of $Ru_3(\mu\text{-dppe})(CO)_{10}$ and $Ru_3(\mu\text{-dppe})_2(CO)_8$ amongst the reaction mixture (analogous to the dppm reaction), together with $\{Ru_3(\mu\text{-H})(\mu\text{-}NC_5H_4)(CO)_9\}_2(\mu\text{-dppe})$ and $Ru_3(\mu\text{-H})(\mu\text{-}NC_5H_4)(\mu\text{-dppe})(CO)_8$; the latter can perhaps be rationalized from the greater flexibility of dppe compared with dppm.

The synthesis of **3** extends the chemistry of the $Ru_3(\mu\text{-dppm})(CO)_{10}$ system. Reactions between $Ru_3(\mu\text{-dppm})(CO)_{10}$ and reagents with a propensity for oxidative addition [RC≡CH (R = Ph, C_6F_5, ^{t}Bu, $SiMe_3$), Au(C≡CPh)(PR'_3) (R′ = Ph, C_6H_4Me-4), I_2 [14], allyl bromide, Me_2S_2, AuCl(PPh_3) [15]] gave products with intact dppm ligands. In the reaction most similar to the present, addition of dihydrogen (H^-/H^+ or H_2) to $Ru_3(\mu\text{-dppm})(CO)_{10}$ gave $Ru_3(\mu\text{-H})(\mu_3\text{-}\eta^2\text{-}PPhCH_2PPh_2)(CO)_9$ [16–19]; as with **3**, the hydride bridges the Ru(1)–Ru(2) bond [20]. The synthesis of **3** is analogous to hydrogenation in that, in both cases, oxidative addition of HX (X = H, NC_5H_4) followed by elimination (of benzene, presumably) occurs under mild conditions to afford the isolated product $Ru_3(\mu_3\text{-}\eta^2\text{-}PPhCH_2PPh_2)(\mu\text{-X})(CO)_{9-n}$ [$n = 0$, X = H; $n = 1$, X = NC_5H_4 (**3**)]. The mild reaction conditions (refluxing acetone) and isolation of unreacted $Ru_3(\mu\text{-dppm})(CO)_{10}$ are consistent with the first step of the reaction being oxidative addition rather than rearrangement of the dppm ligand; no thermolysis product of $Ru_3(\mu\text{-dppm})(CO)_{10}$ [i.e. the orthometalated complex $Ru_3(\mu\text{-H})(\mu_3\text{-}\eta^2\text{-}PPhCH_2PPhC_6H_4)(CO)_9$ [20]] is observed, and oxidative addition of other reagents to $Ru_3(\mu\text{-dppm})(CO)_{10}$ occurs under more forcing conditions (refluxing THF) to give products with an intact dppm ligand. The reason for the elimination step in the formation of **3** [not observed, for example, with $Ru_3(\mu\text{-H})(\mu_3\text{-}\eta^2\text{-}C_2R)(\mu\text{-dppm})(CO)_7$ (see above)] may lie in the location of the bridging hydride in the intermediate; with the acetylide cluster, it is fluxional between the non-dppm bridged edges (*trans*-disposed with respect to the dppm in both cases), whereas in the precursor to **3**, it would be bridging the dppm-bridged edge. It is possible that in this position (*cis*-disposed) it is ideally located to reductively eliminate with a phosphorus bound phenyl to afford **3** (Scheme 1).

4. Experimental

$Ru_3(CO)_{12}$ [21], $Ru_3(\mu\text{-H})(\mu\text{-}NC_5H_4)(CO)_{10}$, $Ru_3(\mu\text{-H})_2(\mu\text{-}NC_5H_4)_2(CO)_8$ [4] and $Ru_3(\mu\text{-dppm})(CO)_{10}$ [22] were synthesized as published. Cyclohexane (sodium) and acetone ($CaCl_2$) were dried and distilled before use. Petrol refers to a mixture of petrols of boiling point range 40–70°C. Pyridine and dppm were obtained commercially (Univar and Aldrich respectively) and used as received. The reactions were carried out using Schlenk techniques [23] under an atmosphere of nitrogen, although subsequent workup was carried

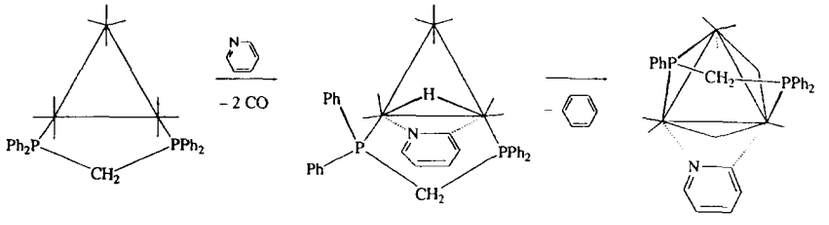

(3)

Scheme 1.

out without any precautions to exclude air. Thin layer chromatography (TLC) was on glass plates (20 × 20 cm) coated with Merck GF_{254} silica gel (0.5 mm).

IR spectra were recorded using a Perkin-Elmer model 1600 Fourier-transform spectrophotometer with CaF_2 optics. ^1H and ^{13}C NMR spectra were recorded on a Varian Gemini spectrometer (300 and 75 MHz respectively, the latter using approximately 0.02 M $Cr(acac)_3$ as the relaxation agent and a recycle delay of 0.5 s). The ^{31}P NMR spectrum was recorded on a Varian XL200E spectrometer (81 MHz). Mass spectra were recorded using a VGZAB 2SEQ instrument (30 kV Cs^+ ions, current 1 mA, accelerating potential 8 kV, 3-nitrobenzyl alcohol matrix) at the Australian National University; peaks were recorded as m/z. Elemental microanalyses were performed by the Microanalysis Service Unit at the University of Queensland.

4.1. Reaction of $Ru_3(\mu\text{-}H)(\mu\text{-}NC_5H_4)(CO)_{10}$ (1) with dppm

Dppm (35 mg, 0.091 mmol) was added to a solution of **1** (60 mg, 0.091 mmol) in cyclohexane (15 ml) and the mixture stirred at 50°C for 16 h. The resulting red–brown solution was taken to dryness and the residue taken up in a minimum amount of CH_2Cl_2. Purification by repeated thin layer chromatography using 30–40% acetone in petrol as eluent afforded a heavy baseline and four major bands from which the products were crystallized (CH_2Cl_2/hexane) and identified as follows:

The first band contained unreacted starting material (**1**; 10 mg, 0.015 mmol, 17%).

The second band afforded orange crystals of $Ru_3(\mu\text{-dppm})(CO)_{10}$ (8 mg, 0.008 mmol, 9%), identified from its IR and ^1H NMR spectra by comparison with the literature [22].

The third band afforded orange crystals identified as $Ru_3(\mu_3\text{-}\eta^2\text{-}PPhCH_2PPh_2)(\mu\text{-}NC_5H_4)(CO)_8$ (**3**, 7 mg, 0.008 mmol, 8%). Anal. Found: C, 41.63; H, 2.26; N, 1.40%; M^+ 915. $C_{32}H_{21}NO_8P_2Ru_3$. Calc.: C, 41.98; H, 2.31; N, 1.53%; M^+ 915. IR (cyclohexane): ν(CO) 2055m, 2010m, 1999s, 1993m,sh, 1981w, 1954w cm^{-1}. ^1H NMR: $\delta(CD_2Cl_2)$ 8.25 (d, J(HH) = 6 Hz, 1H, H6), 7.81–7.30 (m, 17H, Ph + H3), 7.14 (m, 1H, H4), 6.78 (t, J(HH) = 6 Hz, 1H, H5), (aryl H); 3.58, 3.03 (2 × dt, J(HP) = 15 Hz, J(HH) = 5 Hz, 2 × 1H, CH_2). ^{13}C NMR: $\delta(CDCl_3)$ 206.0 (CO); 154.5 (C6), 136.5 (C3), 131.9 (d, J(CP) = 12 Hz), 131.6, 131.2 (d, J(CP) = 11 Hz), 130.5, 130.0, 129.0 (d, J(CP) = 11 Hz), 128.6 (d, J(CP) = 9 Hz), 119.5 (C5) (aryl C). ^{31}P NMR: $\delta(CDCl_3)$ 136.5, 15.3 (2 × d, J(PP) = 134 Hz, PPh, PPh_2).

The fourth band afforded a yellow microcrystalline solid identified as $Ru_3(\mu\text{-dppm})_2(CO)_8$ (4 mg, 0.003 mmol, 3%) by its FAB MS and comparison of its ^1H NMR spectra with the literature. Anal. Found: M^+ 1296. $C_{58}H_{44}O_8P_4Ru_3$ requires M^+ 1296. IR (cyclohexane): ν(CO) 2042m, 1991w, 1973s, 1966s, 1942w cm^{-1}. ^1H NMR: $\delta(CDCl_3)$ 7.29–7.06 (m, 40H, Ph); 4.06 (t, J(HP) = 10 Hz, 4H, CH_2). [Ref. [22] IR (cyclohexane): ν(CO) 2056w, 2046w, 2023m, 2012sh, 1998sh, 1981vs, 1970s, 1945m cm^{-1}. ^1H NMR: $\delta(CDCl_3)$ 7.36 (m, 40H), 4.25 (t, 4H)].

4.2. Reaction of $Ru_3(\mu\text{-dppm})(CO)_{10}$ with pyridine

A mixture of $Ru_3(\mu\text{-dppm})(CO)_{10}$ (500 mg, 0.52 mmol) and pyridine (8.5 g, 0.11 mol) in acetone (50 ml) was heated at reflux for 5 h. The resulting dark brown solution was taken to dryness and taken up in a minimum amount of CH_2Cl_2. Purification by TLC using 2:3 CH_2Cl_2 in petrol as eluent afforded two main yellow bands and a heavy baseline. Band 1 was identified as unreacted $Ru_3(\mu\text{-dppm})(CO)_{10}$ (55 mg, 0.057 mmol, 11%). Band 2 afforded an orange powder from CH_2Cl_2/hexane identified as $Ru_3(\mu_3\text{-}\eta^2\text{-}PPhCH_2PPh_2)(\mu\text{-}NC_5H_4)(CO)_8$ (**3**; 82 mg, 0.090 mmol, 17%).

4.3. Thermolyses of pyridyl-containing clusters

Heating a chlorobenzene (10 ml) solution of $Ru_3(\mu\text{-}H)_2(\mu\text{-}NC_5H_4)_2(CO)_8$ (**2**, 18 mg, 0.026 mmol) for 1 h afforded a black precipitate which was found to be insoluble in acetone.

A similar reaction with $Ru_3(\mu_3\text{-}\eta^2\text{-}PPhCH_2PPh_2)(\mu\text{-}NC_5H_4)(CO)_8$ (**3**, 10 mg, 0.011 mmol) over 16 h afforded a dark brown solution. Attempted purification of the reaction mixture by TLC (1:1 acetone in petrol) afforded a number of trace bands and a heavy baseline.

4.4. Structure determination

Single crystals of compounds **2** and **3** suitable for diffraction analyses were grown from hexane (**2**) and dichloromethane/hexane (**3**) solutions at −30°C. Unique diffractometer data sets were measured at around 295 K within the specified $2\theta_{max}$ limit [$2\theta/\theta$ scan mode; monochromatic Mo K_α radiation ($\lambda = 0.7107_3$ Å)] yielding N independent reflections. N_0 of these with $I > 3\sigma(I)$ were considered "observed" and used in the full matrix least-squares refinement after Gaussian absorption correction. Anisotropic thermal parameters were refined for the non-hydrogen atoms; $(x, y, z, U_{iso})_H$ were refined for the hydrido species and constrained at estimated values for other hydrogens. Conventional residuals R, R_w on $|F|$ at convergence are given, statistical weights derivative of $\sigma^2(I) = \sigma^2(I_{diff}) + 0.0004\sigma^4(I_{diff})$ being used. Neutral atom complex scattering factors were used, computation using the XTAL 3.2 program system [24] implemented by Hall (pertinent results are given in the figures and tables). Lists of atomic coordinates and thermal parameters and a complete list of bond lengths and angles,

have been deposited with the Cambridge Crystallographic Data Centre.

4.4.1. Abnormal features / variations in procedure

Data for **3** were measured with an ω-scan technique in view of the long *b* axis. The coordinated pyridine was indicated as ordered on the basis of refinement behaviour and treated as such. By contrast, for **2**, coordinated pyridine C, N appeared to be disordered in a 50:50 basis over the two possible coordination sites in each case and were refined as composites. It is not possible from the X-ray work to ascertain whether such disorder is concerted, i.e. disorder about Ru(1) being a composite of RuCN and RuNC, exclusive of RuC_2 and RuN_2 components.

Acknowledgements

This work was supported by grants from the Australian Research Council (ARC). Johnson–Matthey Technology Centre is thanked for a generous loan of $RuCl_3$. MPC holds a UNE Postgraduate Research Award and MGH holds an ARC Australian Research Fellowship.

References

[1] M.P. Cifuentes, T.P. Jeynes, M. Gray, M.G. Humphrey, B.W. Skelton and A.H. White, *J. Organomet. Chem.*, *494* (1995) 267.
[2] M.I. Bruce, M.P. Cifuentes and M.G. Humphrey, *Polyhedron*, *10* (1991) 277.
[3] J.R. Katzer and R. Sivasubramanian, *Catal. Rev.-Sci. Eng.*, *25* (1983) 459.
[4] M.I. Bruce, M.G. Humphrey, M.R. Snow, E.R.T. Tiekink and R.C. Wallis, *J. Organomet. Chem.*, *314* (1986) 311.
[5] M.P. Cifuentes, M.G. Humphrey, B.W. Skelton and A.H. White, *J. Organomet. Chem.*, *458* (1993) 211.
[6] M.P. Cifuentes, M.G. Humphrey, B.W. Skelton and A.H. White, *J. Organomet. Chem.*, *466* (1994) 211.
[7] M.P. Cifuentes, M.G. Humphrey, B.W. Skelton and A.H. White, *Organometallics*, *12* (1993) 4272.
[8] A. Eisenstadt, C.M. Giandomenico, M.F. Frederick and R.M. Laine, *Organometallics*, *4* (1985) 2033.
[9] M.D. Curtis, K.R. Han and W.M. Butler, *Inorg. Chem.*, *19* (1980) 2096.
[10] F.A. Cotton, L. Kruczynski and B.A. Frenz, *J. Organomet. Chem.*, *160* (1978) 93.
[11] G. Lavigne, N. Lugan and J.-J. Bonnet, *J. Chem. Soc., Chem. Commun.*, (1987) 957.
[12] N. Lugan, G. Lavigne, J.-J. Bonnet, R. Réau, D. Neilbecker and I. Tkatchenko, *J. Am. Chem. Soc.*, *110* (1988) 5369.
[13] M.P. Cifuentes and M.G. Humphrey, unpublished results.
[14] M.I. Bruce, P.A. Humphrey, E. Horn, E.R.T. Tiekink, B.W. Skelton and A.H. White, *J. Organomet. Chem.*, *429* (1992) 207.
[15] M.I. Bruce, P.A. Humphrey, R.J. Surynt and E.R.T. Tiekink, *Aust. J. Chem.*, *47* (1994) 477.
[16] M.I. Bruce, E. Horn, M.R. Snow and M.L. Williams, *J. Organomet. Chem.*, *276* (1984) C53.
[17] M.I. Bruce, E. Horn, O.b. Shawkataly, M.R. Snow, E.R.T. Tiekink and M.L. Williams, *J. Organomet. Chem.*, *316* (1986) 187.
[18] M.I. Bruce, M.L. Williams, J.M. Patrick, B.W. Skelton and A.H. White, *J. Chem. Soc., Dalton Trans.*, (1986) 2557.
[19] M.I. Bruce, O.b. Shawkataly and M.L. Williams, *J. Organomet. Chem.*, *287* (1985) 127.
[20] N. Lugan, J.-J. Bonnet and J.A. Ibers, *J. Am. Chem. Soc.*, *107* (1985) 4484.
[21] M.I. Bruce, C.M. Jensen and N.L. Jones, *Inorg. Synth.*, *26* (1989) 259.
[22] M.I. Bruce, J.G. Matisons and B.K. Nicholson, *J. Organomet. Chem.*, *247* (1983) 321.
[23] D.F. Shriver and M.A. Drezdzon, *The Manipulation of Air Sensitive Compounds*, Wiley, New York, 1986.
[24] S.R. Hall, H.D. Flack and J.M. Stewart (eds), *The XTAL 3.2 Reference Manual*, Universities of Western Australia, Geneva and Maryland, 1992.
[25] R.H. Fish, T.-J. Kim, J.L. Stewart, J.H. Bushweller, R.K. Rosen and J.W. Dupon, *Organometallics*, *5* (1986) 2193.
[26] R. Zoet, G. van Koten, K. Vrieze, A.J.D. Duisenberg and A.L. Spek, *Inorg. Chim. Acta*, *148* (1988) 71.
[27] A.J. Deeming, R. Peters, M.B. Hursthouse and J.D.J. Backer-Dirks, *J. Chem. Soc., Dalton Trans.*, (1982) 787.
[28] G. Lavigne, N. Lugan and J.-J. Bonnet, *Organometallics*, *1* (1982) 1040.
[29] M.I. Bruce and M.L. Williams, *J. Organomet. Chem.*, *288* (1985) C55.
[30] M.I. Bruce, P.A. Humphrey, B.W. Skelton, A.H. White and M.L. Williams, *Aust. J. Chem.*, *38* (1985) 1301.